Effects of small interfering RNA-mediated hepatic glucagon receptor inhibition on lipid metabolism in *db/db* mice[S]

Seongah Han,[1,*] Taro E. Akiyama,[†] Stephen F. Previs,[*] Kithsiri Herath,[*] Thomas P. Roddy,[*] Kristian K. Jensen,[*] Hong-Ping Guan,[†] Beth A. Murphy,[§] Lesley A. McNamara,[§] Xun Shen,[*] Walter Strapps,[**] Brian K. Hubbard,[*] Shirly Pinto,[*] Cai Li,[†] and Jing Li[1,*]

Division of Cardiovascular Disease,* Diabetes Research,† Pharmacology,§ and RNA Therapeutics,** Merck Sharp & Dohme Corp., Whitehouse Station, NJ

Abstract Hepatic glucose overproduction is a major characteristic of type 2 diabetes. Because glucagon is a key regulator for glucose homeostasis, antagonizing the glucagon receptor (GCGR) is a possible therapeutic strategy for the treatment of diabetes mellitus. To study the effect of hepatic GCGR inhibition on the regulation of lipid metabolism, we generated siRNA-mediated GCGR knockdown (si-GCGR) in the *db/db* mouse. The hepatic knockdown of GCGR markedly reduced plasma glucose levels; however, total plasma cholesterol was increased. The detailed lipid analysis showed an increase in the LDL fraction, and no change in VLDL HDL fractions. Further studies showed that the increase in LDL was the result of over-expression of hepatic lipogenic genes and elevated de novo lipid synthesis. Inhibition of hepatic glucagon signaling via siRNA-mediated GCGR knockdown had an effect on both glucose and lipid metabolism in *db/db* mice.—Han, S., T. E. Akiyama, S. F. Previs, K. Herath, T. P. Roddy, K. Jensen, H-P. Guan, B. A. Murphy, L. A. McNamara, X. Shen, W. Strapps, B. K. Hubbard, S. Pinto, C. Li, and J. Li. **Effects of small interfering RNA-mediated hepatic glucagon receptor inhibition on lipid metabolism in db/db mice. *J. Lipid Res.* 2013.** 54: **2615–2622.**

Supplementary key words diabetes mellitus • glucose • dyslipidemia

Glucagon is a counterregulatory hormone of insulin that has an important physiological role regulating glucose metabolism and preventing hypoglycemia in both animals and humans. The primary target organ of glucagon is liver. Hepatic glucagon receptor and glucagon interaction increases hepatic glucose production by activating glycogenolysis and gluconeogenesis, and abnormal glucagon signaling is associated with hyperglycemia in patients with type 2 diabetes (1). Several preclinical and clinical studies have demonstrated the utility of inhibiting glucagon signaling as one potential strategy for the treatment of type 2 diabetes. For example, pharmacologic or antisense oligonucleotide (ASO) interventions that suppress glucagon receptor signaling have been shown to reverse hyperglycemia in animal models (2–7). Genetic interventions using complete Gcgr knock-out mice also lowered fasting and fed glucose levels with increased GLP-1 and glucagon levels (8–10). More importantly, intervention with glucagon receptor antagonists revealed an impressive circulating plasma glucose-lowering effect in humans (11, 12).

However, concerns over the association between glucagon receptor signaling inhibition and dyslipidemia, specifically, increased LDL-C levels from Gcgr knock-out mice and clinical data using a glucagon receptor antagonist, have been raised (8, 12). Although most studies of glucagon receptor signaling inhibition showed robust glucose lowering, the effects on lipids and the mechanisms linking hepatic glucagon action to LDL-C levels have not been elucidated. The dyslipidemia associated with type 2 diabetes typically involves increased triglycerides (TGs), reduced HDL-C levels, and increased cardiovascular risk (13). Cardiovascular risk is further increased when type 2 diabetes is complicated by elevated LDL-C levels. Thus, it is important to evaluate the impact of hepatic glucagon action inhibition on lipid metabolism, especially hepatic lipid synthesis, TG secretion, and levels of LDL-C and HDL-C. The objective of the present study was to explore the effect of hepatic glucagon receptor ablation on lipid metabolism in a *db/db* diabetic mouse model.

Funding for this study was provided by Merck Sharp & Dohme Corp., a subsidiary of Merck & Co., Inc., Whitehouse Station, NJ. All authors are current or former employees of Merck Sharp & Dohme Corp., a subsidiary of Merck & Co., Inc., Whitehouse Station, NJ, and may own stock or have stock options in the company.

Manuscript received 31 December 2012 and in revised form 14 May 2013.

Published, JLR Papers in Press, July 4, 2013
DOI 10.1194/jlr.M035592

Copyright © 2013 by the American Society for Biochemistry and Molecular Biology, Inc.

Abbreviations: ASO, antisense oligonucleotide; BHB, β hydroxybutylate; FPLC, fast protein liquid chromatography; NEFA, nonesterified fatty acid; siRNA, small interfering RNA; TG, triglyceride.

[1] To whom correspondence should be addressed.
e-mail: jing_li4@merck.com (J.L.); Seongah_Han@merck.com (S.H.)

[S] The online version of this article (available at http://www.jlr.org) contains supplementary data in the form of three figures.

MATERIALS AND METHODS

Animal study

Male, 8 week-old *db/db* mice were purchased from The Jackson Laboratory (Bar Harbor, ME) and fed a regular chow diet (Diet 7012; Harlan Teklad) throughout the study. Following a 2 week stabilizing period, 10 week-old mice were used for small interfering RNA (siRNA) injection. siRNA was packaged in lipid nanoparticles, as previously described (14). Chemically modified siRNAs were synthesized and characterized, as previously described (14).

5′-UGGUCAAGUGUCUGUUUGA-3′and 5′-GGACTTCTCTC-AATTTTCT-3′ were siRNA target sequences for Gcgr and a nontargeting control siRNA, respectively. The encapsulated siRNAs were injected via tail vein in a 3 mg/kg dose on days 0 and 6. Animals were euthanized at day 11, and blood and liver samples were collected immediately following euthanasia. Animal procedures were practiced in conformity with Public Health Service policy and the guidelines of the Institutional Animal Care and Use Committee of Merck.

Plasma characterization of metabolic phenotypes, and hepatic lipid determination

Ambient (nonfasted) plasma glucose levels were measured at 9:00 AM from tail bleeds with a glucometer (One Touch Ultra; LifeScan, Inc., Milpitas, CA) at day 4 and day 11 after siRNA injection. At day 11, mice were fasted for 5 h, and blood samples were collected. Plasma was separated by centrifugation and stored at −80°C until analysis. Total plasma cholesterol and HDL-C were measured using commercial kits (Wako Chemicals; Richmond, VA) according to the manufacturers' protocol. Plasma insulin and TG levels were measured using an ALPCO ELISA kit (ALPCO Diagnostics; Salem, NH) and the Infinity Triglycerides kit (Thermo Fisher Scientific; Waltham, MA), respectively, according to the manufacturers' instructions. Glucagon was measured using commercial ELISA kits (Linco Research Immunoassay; St. Charles, MO). Nonesterified fatty acid (NEFA) was measured using commercially available enzyme-coupled spectrophotometric assays (Wako Chemicals, Inc.), and β hydroxybutylate (bHB) was measured using the Liquid Enzymatic Reagent Kit (Stanbio Laboratory; Boerne, TX). Plasma apoB and apoA-I levels were measured by LC/MS assay, and protein convertase subtilisin/kexin type 9 (PCSK9) was measured using murine-specific ELISA, as previously described (14, 15). All assays were performed following the recommended procedures for instrument operation, calibration, quality control, and assay guidelines. Hepatic TG and cholesterol content were measured as previously described (16).

Western blot analysis

To examine expression of proteins, liver samples were collected and cell lysates were prepared as described previously (16). Western blot analysis was carried out as described earlier (16) using anti-Ldlr antibody (Abcam, PLC; Waltham, MA) and anti-α tubulin (Abcam, PLC).

Lipoprotein separation and TG production

The major lipoproteins (VLDL-C; d < 1.006 g/ml), LDL-C (d = 1.006–1.063 g/ml), and HDL-C (d = 1.063–1.21 g/ml) were isolated by sequential density ultracentrifugation of plasma using a TLA-100 rotor (Beckman Coulter, Inc.; Brea, CA), following procedures described previously (16). Sodium bromide (NaBr) (Sigma-Aldrich, St. Louis, MO) was used to prepare the density solution. ApoB-containing lipoproteins were run on SDS-PAGE gels and visualized by 0.05% Coomassie blue staining (Sigma-Aldrich). P407 (Pluronic F-127; Invitrogen, Grand Island, NY) was used in mice to measure TG production rate in plasma. Mice were fasted overnight and injected with P407 (10 ml/kg body weight). Blood samples were collected at 0, 1, 2, 4, and 6 h after injection, and TG levels were quantified, as described above.

Fast protein liquid chromatography

Lipoproteins were fractionated by fast protein liquid chromatography (FPLC) gel filtration using a Superose-6 size exclusion column (GE Healthcare LifeSciences, Inc.; Piscataway, NJ) attached to a Dionex HPLC system (Thermo Fisher Scientific, Inc.). The column effluent was mixed with a commercially available enzymatic reagent for cholesterol (Wako Chemicals), and levels were continuously measured using a photodiode array detector at 600 nm absorbance. The first, second, and third peaks were attributed to VLDL, LDL-C, and HDL-C, respectively, and the area under each peak was calculated using Chromeleon software, as previously described (17).

Real-time quantitative PCR analysis

Liver samples were homogenized, and total RNA was isolated using RNA Easy (Qiagen, Inc., Valencia, CA), according to the manufacturer's instructions. Two micrograms total RNA from each sample was reverse transcribed with a cDNA kit (Life Technologies Corp., Carlsbad, CA), and mRNA expression for the genes of interest was measured by RT-PCR, with SYBR Green PCR core reagents and primers (Qiagen, Inc.), as previously described (18). The relative amounts of specific target amplicons for each primer set were estimated by a cycle threshold (Ct) value and were normalized to the copy number of housekeeping genes (18). The *P* values were determined by two-tailed equal variance Student's *t*-test, comparing the ΔCt values of the si-Control and si-GCGR groups.

GC-quadrupole-MS analyses of palmitate and cholesterol synthesis

At day 11 after siRNA injection, ^2H_2O (Sigma-Aldrich) was injected at 20 ml/kg body weight into animals that had been fasted 4 h. Plasma samples were collected after 4 h of tracer incorporation, and stored at −80°C until analysis. Total plasma (35 μl) was spiked with a known amount of heptadecanoic acid (C17:0, internal standard) and then saponified in 1 N potassium hydroxide (KOH) in 80% ethanol (heated at 65°C for 60 minutes). Samples were acidified (25 μl 6 N hydrochloric acid (HCl), and the lipids were then extracted with chloroform. Following evaporation of the solvent, the residue was first reacted with trimethylsilyldiazomethane to form FA methyl esters, evaporated to dryness, and then reacted with pyridine-acetic anhydride (1:1, v/v) at 65°C for 30 min to generate cholesterol acetate. The reagents were evaporated to dryness. The ^2H labeling of the derivatized lipids was determined using an Agilent 5973N-MSD equipped with an Agilent 6890 GC system (Agilent Technologies; Santa Clara, CA), a DB5-MS capillary column (30 m × 0.25 mm × 0.25 μm). The mass spectrometer was operated in the electron impact mode, using selective ion monitoring of *m/z* 270 and 271 for palmitate, 284 and 285 for C17:0 (internal standard), and 368 and 369 for cholesterol; data were collected using selected ion monitoring at a dwell time of 10 ms per ion. To quantify the contribution of lipid synthesis, a precursor product labeling ratio was assumed and the general equation was used:

$$\%\ \text{newly made material} = \text{product labeling}/(\text{precursor labeling} \times n) \times 100 \qquad \textit{Eq. 1}$$

for which product labeling = palmitate or cholesterol, precursor labeling = body water, and n = the number of exchangeable

hydrogens (assumed to equal 22 and 25 for palmitate and cholesterol, respectively) (19, 20).

Statistics

Values are expressed as means ± SEM. The statistical significance of the differences was determined by Student's *t*-test, and a *P* value <0.05 was considered significant.

RESULTS

Hepatic GCGR knockdown lowered plasma glucose levels

Eleven days after siRNA injection, a reduction in hepatic Gcgr mRNA expression (61%) in si-GCGR mice was observed (**Fig. 1A**). There was no difference in cumulative body weight in the si-GCGR group compared with the control group throughout the study (Fig. 1B). Compared with si-Control mice, both ambient and fasting glucose levels in si-GCGR-treated mice were reduced at day 4, and the reduction was sustained to day 11 after treatment (Fig. 1C, D). Although plasma glucagon levels were elevated in the si-GCGRsi-GCGR-treated mice, plasma insulin levels were similar in the two groups (Fig. 1E, F).

The effect of hepatic GCGR knockdown on plasma lipid levels

Lipoprotein analysis showed a 2-fold increase of LDL-C levels in si-GCGR-treated mice compared with those in the si-Control group, with no significant difference in VLDL and HDL-C levels (**Fig. 2A**). In addition, there were no differences in hepatic LDL receptor expression, plasma PCSK9 levels, or lipoprotein lipase activity between these two groups (Fig. 2B, C; see supplementary Fig. IA). The use of ultracentrifugation to isolate lipoprotein fractions revealed a slight increase in apoB-100 content in LDL fractions, with a tendency toward increased total plasma apoB levels in si-GCGR mice (Fig. 2D, E). FPLC separation confirmed an increase of LDL-C fraction in si-GCGR mice (Fig. 2F).

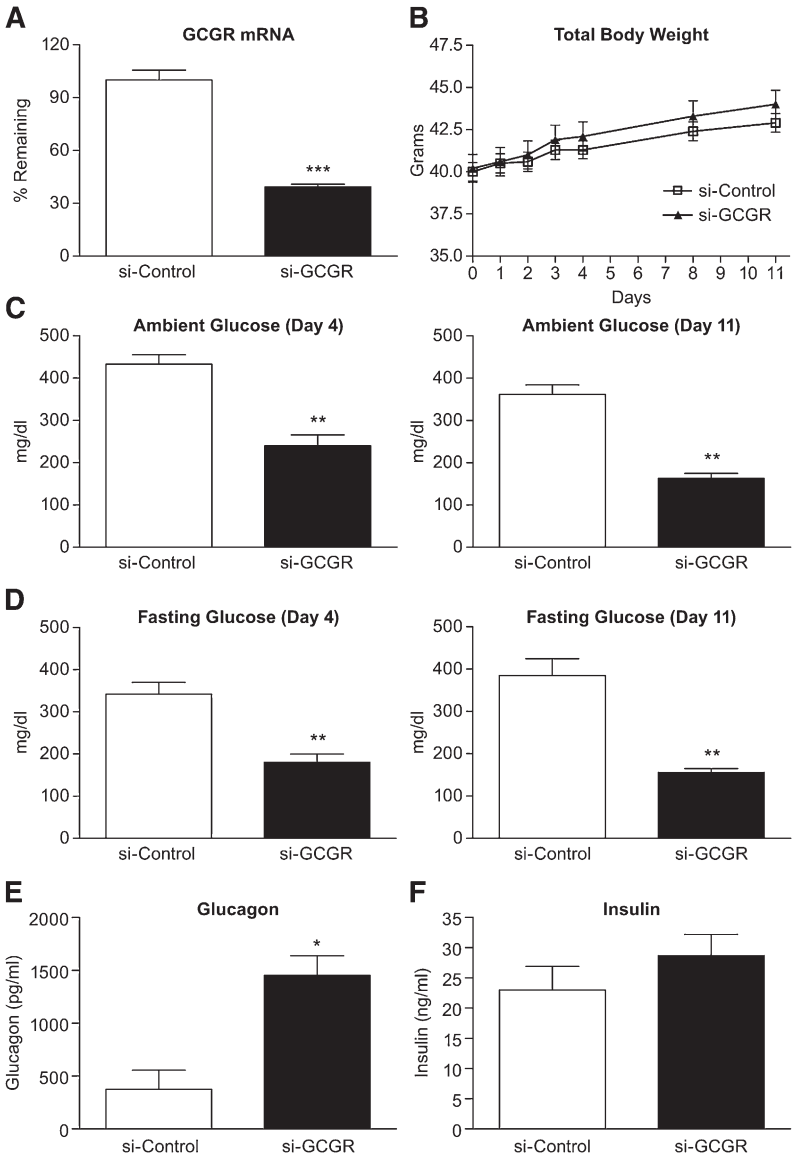

Fig. 1. Effect of hepatic GCGR knockdown on hepatic GCGR mRNA, body weight, and plasma glucose, glucagon and insulin levels in *db/db* mice. Mice were injected with GCGR siRNA and euthanized 11 days after injection. A: Hepatic Gcgr mRNA expression by real-time quantitative PCR in si-Control and si-GCGR. B: Body weight at 1, 2, 3, 4, 8, and 11 days after siRNA injection in si-Control and si-GCGR mice. Ambient glucose (C), fasting glucose (D), glucagon (E), and insulin levels (F) measured in si-Control and si-GCGR mice plasma samples. Values are expressed as means ± SEM (n = 7–8). The statistical significance of the differences was determined by Student's *t*-test, and a *P* value <0.05 was considered significant (**P* < 0.05; **<0.01 vs. si-Control).

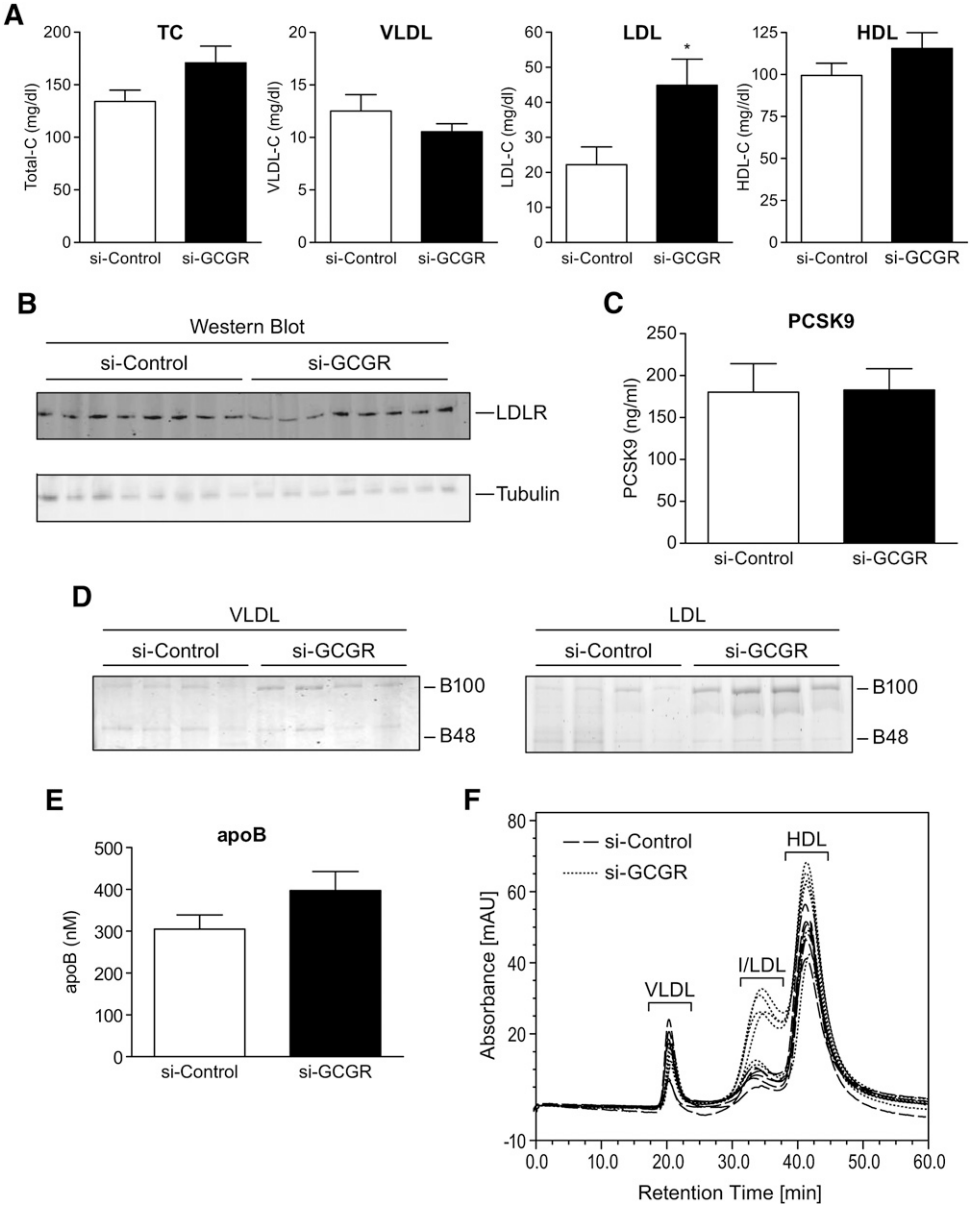

Fig. 2. Plasma lipoprotein analysis of si-Control and si-GCGR-treated *db/db* mice. A: Quantification of plasma TC, VLDL-C, LDL-C, and HDL-C from si-Control and si-GCGR-injected mice. B: Western blot analysis of LDLR protein levels in liver tissues from si-Control and si-GCGR mice. C: Quantification of plasma PCSK9 levels in si-Control and si-GCGR mice. D: Representative sample of apoB-100 and apoB-48 levels shown in A. Ultracentrifugation-isolated apoB-containing lipoproteins in VLDL(left panel) and LDL(right panel) were resolved by SDS-PAGE and visualized by Coomassie blue staining. E: Quantification of plasma apoB levels in si-Control and si-GCGR mice. F: Lipoprotein separation by FPLC. Plasma samples from si-Control and si-GCGR-injected mice. The results given in figures A, C, and E are shown as means ± SEM (n = 8). The statistical significance of the differences was determined by Student's *t*-test, and a *P* value <0.05 was considered significant (**P* < 0.05 vs. si-Control). TC, total cholesterol; VLDL-C, VLDL cholesterol; LDL-C, LDL cholesterol; HDL-C, HDL cholesterol.

Hepatic GCGR knockdown mice showed increased hepatic lipid contents and lipogenic gene expression

There were increased levels of TGs and cholesterol in the liver samples from si-GCGR mice (**Fig. 3A**). This increase may have potentially resulted from increased expression of hepatic lipogenic genes. There was no differential expression of sterol-regulatory element-binding protein isoform-1c (Srebf1) or SREBP-2 (Srebf2) mRNA in fed liver samples from si-GCGR mice compared with controls (Fig. 3B). However, we observed a profound increase in the expression of genes in SREBP pathways, such as FA synthase (Fasn), acetyl-CoA carboxylase A and B (Acaca, Acacb), stearoyl-CoA desaturase (Scd1), elongation of very long-chain fatty acids protein (Elovl5, Elovl6), long-chain-fatty acid-CoA ligase (Acsl3, Acsl5), Acyl-CoA synthetase short-chain family member 2 (Acss2), ATP citrate lyase (Acly), acetoacetyl-CoA synthetase (Aacs), mevalonate decarboxylase (Mvd), and farnesyl diphosphate

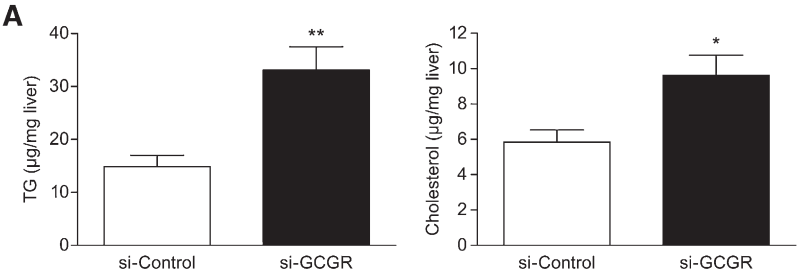

B

Gene Symbol	Fold Regulation	*P*-value	Gene Symbol	Fold Regulation	*P*-value
Fasn	3.4	0.0005	Mttp	1.2	0.0226
Acaca	1.7	0.0054	ApoB	1.1	0.1500
Acacb	1.4	0.0354	Lpl	1.0	0.6386
Scd1	2.5	0.0028	PCSK9	1.1	0.7678
Elovl5	1.4	0.0030	Ldlr	1.2	0.2528
Elovl6	2.8	0.0014	Gck	1.6	0.0214
Acsl3	1.6	0.0124	Pklr	1.5	0.0136
Acsl5	2.0	0.0282	Pepck	0.5	0.0037
Acss2	1.7	0.0415	Srebf1	1.0	0.9870
Acly	2.0	0.0041	Srebf2	1.1	0.5124
Aacs	1.9	0.0169	Hmgcr	1.8	0.0743
Mvd	1.3	0.0233	Chrebp	1.0	0.8960
Fdps	1.6	0.0320			

Fig. 3. Hepatic lipid content and mRNA expression of genes involved in lipid metabolism. A: Hepatic TG and cholesterol levels in the livers of si-Control and si-GCGR mice. Data are shown as the mean ± SEM (n = 8). The statistical significance of the differences was determined by Student's *t*-test, and a *P* value <0.05 was considered significant (**P*< 0.05; **<0.01 vs. si-Control). B: Analysis of hepatic gene expression by real-time quantitative PCR in si-Control and si-GCGR mice (n = 8). Fold regulation indicates the ratio of expression levels in si-GCGR over si-Control. Livers were collected from mice in the fed condition. The statistical significance of the differences was determined by Student's *t*-test, and a *P* value <0.05 was considered significant.

synthetase (Fdps) (Fig. 3B). A tendency of increased expression was shown by 3-hydroxy-3-methylglutaryl-CoA reductase (Hmgcr), whereas MLX interactor (Chrebp) mRNA expression was unchanged (Fig. 3B). Microsomal triglyceride transfer protein (Mttp) showed a moderate increase in expression, whereas other potential candidate molecules involved in the regulation of apoB-containing lipoprotein levels, including apoB, Lpl, PCSK9, or Ldlr mRNA expression, were unchanged (Fig. 3B). As expected with inhibition of glucagon signaling, the expression of glucokinase (Gck) and pyruvate kinase (Pklr) was increased, and the expression of phosphoenolpyruvate carboxykinase (Pepck) was decreased in the hepatic Gcgr knockdown mice group (Fig. 3B). Upregulation of lipogenic and glycogen biosynthetic genes and reduction of gluconeogenic gene expression were observed with hepatic Gcgr knockdown. These findings suggest that reduced levels of hepatic glucagon receptor in *db/db* mice produce an upregulation of lipogenic genes, which may eventually lead to increased hepatic lipid contents.

Hepatic GCGR knockdown mice showed increased de novo lipid synthesis and TG secretion

Stable isotope tracer studies were performed to determine whether increased expression of hepatic lipogenic genes translated into increased lipid synthesis in si-GCGR mice. To quantify the rate of de novo lipogenesis, both groups of mice were injected with ^2H_2O tracer, and the ^2H labeling of cholesterol and palmitate was quantified using GC/MS. A significant increase in the synthesis of cholesterol (>2-fold) and palmitate (>5-fold) was observed in si-GCGR-treated groups relative to controls (**Fig. 4A, B**). Presumably, changes in the production of these plasma lipids reflect hepatic metabolism, because the liver is a major source of newly made circulating lipids. To determine whether these changes lead to altered hepatic lipoprotein secretion, the lipase inhibitor P407 was administered by injection to both groups of mice. P407 blocks the clearance of apoB-containing lipoproteins from the circulation; thus, the rate of accumulation of lipoprotein reflects the secretion rate in plasma. The results showed an increase in hepatic secretion of TGs in si-GCGR mice as well as increased basal plasma TG levels (Fig. 4C, D). Compared with control groups, there was no difference in plasma levels of NEFA, bHB, alanine transaminase, and aspartate aminotransferase in the si-GCGR group (Fig. 4E, F; see supplementary Fig. IB).

DISCUSSION

Targeting glucagon action to treat type 2 diabetes has been of great interest. This study demonstrated a strong and sustained effect on glucose lowering in siRNA-mediated hepatic Gcgr knockdown in *db/db* mice. Previous studies have shown that inhibiting glucagon action improves glycemic control in animals and humans (9, 11, 12, 21). Consistent with those observations, the present results

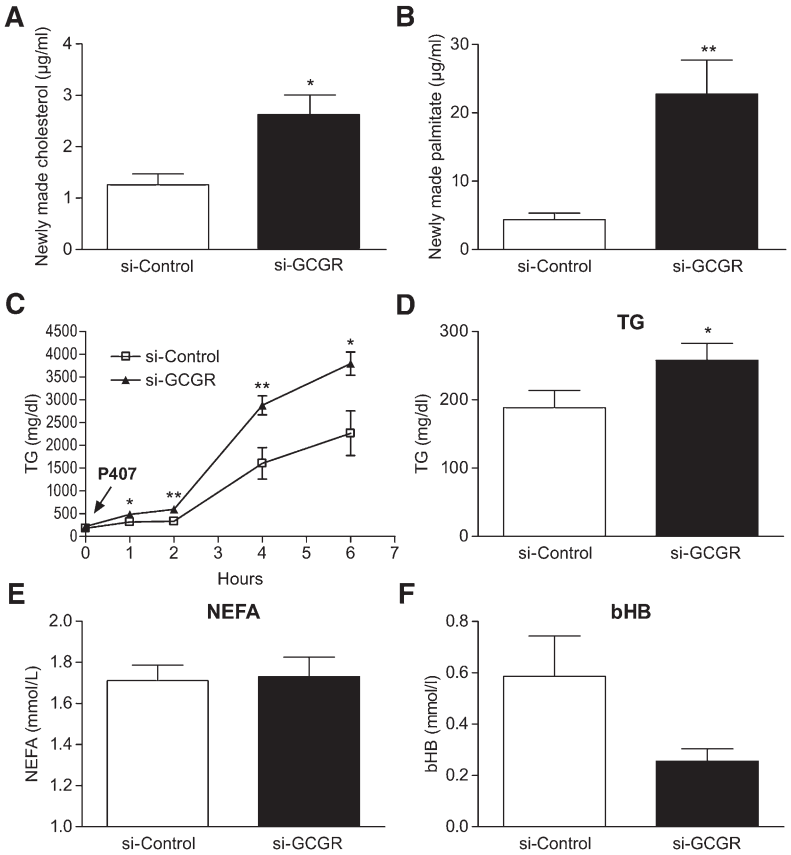

Fig. 4. Cholesterol and palmitate synthesis and TG production. Newly synthesized cholesterol (A) and palmitate (B) of si-Control and si-GCGR-injected mice. C: TG production in si-Control and si-GCGR mice. TG production was determined by measuring plasma TG concentrations at indicated times after P407 injection. Quantifications of plasma levels of TG (D), NEFA (E), and β hydroxybutylate (bHB) (F) from si-Control and si-GCGR mice. All values are expressed as means ± SEM (n = 6–8). The statistical significance of the differences was determined by Student's *t*-test, and a *P* value <0.05 was considered significant (**P* < 0.05; **<0.01 vs. si-Control).

indicate that blocking GCGR activation can improve glucose control in a diabetic mouse model.

Although such therapies have consistently demonstrated improvement of glucose in different mouse models and even human clinical trials, questions regarding the potential effects of blocking glucagon action on lipid metabolism have been raised. Interestingly, several other studies have also illustrated the potential hypolipidemic actions of glucagon, specifically, with respect to reduced plasma TG, VLDL secretion, hepatic TG contents, cholesterol levels, and increased FA oxidation (22–25). These findings underscore the importance of understanding the potential implications of downregulating glucagon signaling on lipid metabolism.

Previously published studies examining GCGR inhibition revealed somewhat inconsistent results with respect to lipid effects, insofar as not all $Gcgr^{-/-}$ mice or GCGR ASO-treated mice exhibited dyslipidemic phenotypes (5, 6, 8, 9, 23). In some studies, $Gcgr^{-/-}$ mice showed increased plasma LDL or total cholesterol levels, but no increased (or even reduced) plasma TG levels (8, 9). In another study, $Gcgr^{-/-}$ mice showed increased TG secretion and increased plasma TG levels after a 16 h fast (23). GCGR ASO-treated *db/db* mice showed reduced plasma TG levels and increased hepatic TG contents (5, 6).

In the current study, inhibition of GCGR by si-RNA demonstrated effects on both glucose and lipid metabolism in the *db/db* mouse model. The si-GCGR *db/db* mouse showed robust glucose lowering and increased LDL-C levels. Si-GCGR mice showed increased hepatic lipid contents, lipogenic gene expression, and TG production. All of these aggravated dyslipidemic characteristics are associated with an upregulation of de novo lipogenesis. We did not observe any increase in plasma NEFA concentrations to suggest increased FA flux to liver, nor a reduction in β-hydroxybutyrate levels and/or reduction in the expression of FA oxidation genes in si-GCGR mice (Fig. 4E, F; data not shown). Hepatic LDLR protein and plasma PCSK9 levels were also unchanged; therefore, the increasing LDL-C is probably less due to the reduction in LDL fractional catabolism. On the basis of our results, we propose that the elevated rate of lipogenesis is a major driving force for the observed increases in LDL-C levels and increased TG production in si-GCGR *db/db* mice. Interestingly, siRNA-mediated knock down of fructose-1,6-bisphosphatase 1, which converts fructose 1,6 biphosphate to fructose 6-phosphate in gluconeogenesis, also reduced plasma glucose levels, increased LDL-C levels, and upregulated expression of hepatic lipogenic gene expression in the *db/db* mouse model (see supplementary Fig. II; data not shown).

We also tested the effect of knockdown glucagon receptor in a mouse model without impairment of leptin signaling, CETP transgenic $LDLR^{+/-}$ mouse, using siRNA targeting Gcgr. The si-GCGR-treated mice showed ~20% reduction in plasma glucose and ~24% induction of LDL-C levels in the CETP-transgenic $LDLR^{+/-}$ mouse model (see supplementary Fig. III).

The inhibition of hepatic gluconeogenesis and possible increase in glycolysis in si-GCGR mice could lead to

build-up of acetyl-CoA, which can be used as carbon substrate for lipid synthesis. The newly synthesized hepatic lipid can be either stored or secreted as VLDL. Certainly, we observed increased hepatic lipid contents as well as increased TG production. Another explanation could be that knocking down GCGR sensitized the liver to insulin-mediated lipogenesis. It is well documented that insulin upregulates FA biosynthesis and glycolysis genes. One study showed inhibitory effects of glucagon on hepatic lipogenesis by antagonizing the signaling pathway mediated by insulin (26). A recent study showed a global upregulation of lipid biosynthesis and glycolysis genes in $Gcgr^{-/-}$ mice liver at both mRNA and protein levels (27). Importantly, Gcgr knockout or Gcgr monoclonal antibody-treated preclinical animal models showed elevated plasma cholesterol and LDL cholesterol (8, 28), which might be caused by increased hepatic cholesterol synthesis. Indeed, our stable isotope tracer studies demonstrated that cholesterol synthesis (^{2}H labeling of cholesterol) was significantly increased in si-GCGR-treated mice. It is interesting to note that we did not observe robust change of gene expressions involved in cholesterol synthesis, which is somewhat inconsistent with the report that multiple genes of cholesterol biosynthesis were elevated in $Gcgr^{-/-}$ mice (27). This discrepancy might be due to differences in the genetic background, the dysmetabolic status of mice, and the degree of GCGR deficiency. The implications of these findings could be that glucagon/GCGR signaling not only plays a role in glucose metabolism but also protects against excessive hepatic lipid production.

Given that increased atherosclerosis is a major cause of morbidity and mortality in type 2 diabetes and metabolic syndrome (29), it is important to carefully evaluate the potential association of increased LDL cholesterol levels when GCGR is antagonized. The current study demonstrated the potential association between hepatic glucagon signaling and regulation of lipogenesis and plasma LDL in the *db/db* mouse model. Although there may be concerns with respect to directly applying results from a mouse model to human lipid metabolism, the hepatic Gcgr knockdown in *db/db* mice is a useful model by which to study the interaction of hepatic glucagon signaling and lipid metabolism. Whether the glucose and lipid effects can be decoupled at the glucagon receptor level will be of great interest to the field. Understanding the glucagon/GCGR mechanisms that control lipid metabolism will provide important insights to guide the design of the next generation of GCGR antagonists for the treatment of type 2 diabetes.

The authors thank Christine McCrary Sisk and Kathleen Newcomb of Merck Sharp & Dohme Corp., for their editorial assistance in the preparation of this manuscript and Xun Shen of Merck Sharp & Dohme Corp. for generating the Western blot analysis data set.

REFERENCES

1. D'Alessio, D. 2011. The role of dysregulated glucagon secretion in type 2 diabetes. *Diabetes Obes. Metab.* **13 (Suppl.):** 126–132.
2. Petersen, K. F., and J. T. Sullivan. 2001. Effects of a novel glucagon receptor antagonist (Bay 27–9955) on glucagon-stimulated glucose production in humans. *Diabetologia.* **44:** 2018–2024.
3. Qureshi, S. A., C. M. Rios, D. Xie, X. Yang, L. M. Tota, V. D. Ding, Z. Li, A. Bansal, C. Miller, S. M. Cohen, et al. 2004. A novel glucagon receptor antagonist inhibits glucagon-mediated biological effects. *Diabetes.* **53:** 3267–3273.
4. Winzell, M. S., C. L. Brand, N. Wierup, U. G. Sidelmann, F. Sundler, E. Nishimura, and B. Ahren. 2007. Glucagon receptor antagonism improves islet function in mice with insulin resistance induced by a high-fat diet. *Diabetologia.* **50:** 1453–1462.
5. Sloop, K. W., J. X. Cao, A. M. Siesky, H. Y. Zhang, D. M. Bodenmiller, A. L. Cox, S. J. Jacobs, J. S. Moyers, R. A. Owens, A. D. Showalter, et al. 2004. Hepatic and glucagon-like peptide-1-mediated reversal of diabetes by glucagon receptor antisense oligonucleotide inhibitors. *J. Clin. Invest.* **113:** 1571–1581.
6. Liang, Y., M. C. Osborne, B. P. Monia, S. Bhanot, W. A. Gaarde, C. Reed, P. She, T. L. Jetton, and K. T. Demarest. 2004. Reduction in glucagon receptor expression by an antisense oligonucleotide ameliorates diabetic syndrome in db/db mice. *Diabetes.* **53:** 410–417.
7. Sørensen, H., C. L. Brand, S. Neschen, J. J. Holst, K. Fosgerau, E. Nishimura, and G. I. Shulman. 2006. Immunoneutralization of endogenous glucagon reduces hepatic glucose output and improves long-term glycemic control in diabetic ob/ob mice. *Diabetes.* **55:** 2843–2848.
8. Gelling, R. W., X. Q. Du, D. S. Dichmann, J. Romer, H. Huang, L. Cui, S. Obici, B. Tang, J. J. Holst, C. Fledelius, et al. 2003. Lower blood glucose, hyperglucagonemia, and pancreatic alpha cell hyperplasia in glucagon receptor knockout mice. *Proc. Natl. Acad. Sci. USA.* **100:** 1438–1443.
9. Parker, J. C., K. M. Andrews, M. R. Allen, J. L. Stock, and J. D. McNeish. 2002. Glycemic control in mice with targeted disruption of the glucagon receptor gene. *Biochem. Biophys. Res. Commun.* **290:** 839–843.
10. Conarello, S. L., G. Jiang, J. Mu, Z. Li, J. Woods, E. Zycband, J. Ronan, F. Liu, R. S. Roy, L. Zhu, et al. 2007. Glucagon receptor knockout mice are resistant to diet-induced obesity and streptozotocin-mediated beta cell loss and hyperglycaemia. *Diabetologia.* **50:** 142–150.
11. Kelly, R. P., P. Garhyan, E. J. Abu-Raddad, H. Fu, C. Lim, M. J. Prince, J. A. Pinaire, M. Loh, and M. A. Deeg. 2011. Short-term treatment with glucagon receptor antagonist LY2409021 effectively reduces fasting blood glucose (FBG) and HbA1c in patients with type 2 diabetes mellitus (T2DM) [abstract]. *Diabetes.* **60 (Suppl.):** A84.
12. Engel, S. S., L. Xu, P. J. Andryuk, M. J. Davies, J. Amatruda, K. Kaufman, and B. J. Goldstein. 2011. Efficacy and tolerability of MK-0893, a glucagon receptor antagonist (GRA), in patients with type 2 diabetes (T2DM) [abstract]. *Diabetes.* **(Suppl.):** A85.
13. Krauss, R. M. 2004. Lipids and lipoproteins in patients with type 2 diabetes. *Diabetes Care.* **27:** 1496–1504.
14. Tadin-Strapps, M., L. B. Peterson, A. M. Cumiskey, R. L. Rosa, V. H. Mendoza, J. Castro-Perez, O. Puig, L. Zhang, W. R. Strapps, S. Yendluri, et al. 2011. siRNA-induced liver ApoB knockdown lowers serum LDL-cholesterol in a mouse model with human-like serum lipids. *J. Lipid Res.* **52:** 1084–1097.
15. Chen, Z., S. P. Wang, M. L. Krsmanovic, J. Castro-Perez, K. Gagen, V. Mendoza, R. Rosa, V. Shah, T. He, S. J. Stout, et al. 2012. Small molecule activation of lecithin cholesterol acyltransferase modulates lipoprotein metabolism in mice and hamsters. *Metabolism.* **61:** 470–481.
16. Han, S., C. P. Liang, M. Westerterp, T. Senokuchi, C. L. Welch, Q. Wang, M. Matsumoto, D. Accili, and A. R. Tall. 2009. Hepatic insulin signaling regulates VLDL secretion and atherogenesis in mice. *J. Clin. Invest.* **119:** 1029–1041.
17. Han, S., A. M. Flattery, D. McLaren, R. Raubertas, S. H. Lee, V. Mendoza, R. Rosa, N. Geoghagen, J. M. Castro-Perez, T. P. Roddy, et al. 2012. Comparison of lipoprotein separation and lipid analysis methodologies for human and cynomolgus monkey plasma samples. *J. Cardiovasc. Transl. Res.* **5:** 75–83.
18. Jensen, K. K., S. F. Previs, L. Zhu, K. Herath, S. P. Wang, G. Bhat, G. Hu, P. L. Miller, D. G. McLaren, M. K. Shin, et al. 2012. Demonstration of diet-induced decoupling of fatty acid and cholesterol synthesis by combining gene expression array and 2H2O quantification. *Am. J. Physiol. Endocrinol. Metab.* **302:** E209–E217.
19. Lee, W. N., S. Bassilian, H. O. Ajie, D. A. Schoeller, J. Edmond, E. A. Bergner, and L. O. Byerley. 1994. In vivo measurement of fatty acids and cholesterol synthesis using D2O and mass isotopomer analysis. *Am. J. Physiol.* **266:** E699–E708.

20. Diraison, F., C. Pachiaudi, and M. Beylot. 1996. In vivo measurement of plasma cholesterol and fatty acid synthesis with deuterated water: determination of the average number of deuterium atoms incorporated. *Metabolism.* **45:** 817–821.
21. Mu, J., G. Jiang, E. Brady, Q. Dallas-Yang, F. Liu, J. Woods, E. Zycband, M. Wright, Z. Li, K. Lu, et al. 2011. Chronic treatment with a glucagon receptor antagonist lowers glucose and moderately raises circulating glucagon and glucagon-like peptide 1 without severe alpha cell hypertrophy in diet-induced obese mice. *Diabetologia.* **54:** 2381–2391.
22. Eaton, R. P. 1973. Hypolipemic action of glucagon in experimental endogenous lipemia in the rat. *J. Lipid Res.* **14:** 312–318.
23. Longuet, C., E. M. Sinclair, A. Maida, L. L. Baggio, M. Maziarz, M. J. Charron, and D. J. Drucker. 2008. The glucagon receptor is required for the adaptive metabolic response to fasting. *Cell Metab.* **8:** 359–371.
24. Xiao, C., M. Pavlic, L. Szeto, B. W. Patterson, and G. F. Lewis. 2011. Effects of acute hyperglucagonemia on hepatic and intestinal lipoprotein production and clearance in healthy humans. *Diabetes.* **60:** 383–390.
25. Aubry, F., Y. L. Marcel, and J. Davignon. 1974. Effects of glucagon on plasma lipids in different types of primary hyperlipoproteinemia. *Metabolism.* **23:** 225–238.
26. Xiong, Y., Q. F. Collins, J. An, E. Lupo, Jr., H. Y. Liu, D. Liu, J. Robidoux, Z. Liu, and W. Cao. 2007. p38 mitogen-activated protein kinase plays an inhibitory role in hepatic lipogenesis. *J. Biol. Chem.* **282:** 4975–4982.
27. Yang, J., M. L. MacDougall, M. T. McDowell, L. Xi, R. Wei, W. J. Zavadoski, M. P. Molloy, J. D. Baker, M. Kuhn, O. Cabrera, et al. 2011. Polyomic profiling reveals significant hepatic metabolic alterations in glucagon-receptor (GCGR) knockout mice: implications on anti-glucagon therapies for diabetes. *BMC Genomics.* **12:** 281.
28. Gu, W., H. Yan, K. A. Winters, R. Komorowski, S. Vonderfecht, L. Atangan, G. Sivits, D. Hill, J. Yang, V. Bi, et al. 2009. Long-term inhibition of the glucagon receptor with a monoclonal antibody in mice causes sustained improvement in glycemic control, with reversible alpha-cell hyperplasia and hyperglucagonemia. *J. Pharmacol. Exp. Ther.* **331:** 871–881.
29. Nigro, J., N. Osman, A. M. Dart, and P. J. Little. 2006. Insulin resistance and atherosclerosis. *Endocr. Rev.* **27:** 242–259.